Polysynthetic Twinning in Poly(vinylcyclohexane) Single Crystals and "Fractional" Secondary Nucleation in Polymer Crystal Growth

Daniel Alcazar,[†] Jrjeng Ruan,[†,‡] Annette Thierry,[†] Akiyoshi Kawaguchi,[§] and Bernard Lotz*,[†]

Institut Charles Sadron (CNRS-ULP), 6 Rue Boussingault, 67083 Strasbourg, France, and Faculty of Science and Engineering, Ritsumeikan University, Noji-Higashi, Kusatsu, Shiga 525-8577, Japan

Received October 28, 2005; Revised Manuscript Received November 12, 2005

ABSTRACT: The internal structure of single crystals and twinned crystals of isotactic poly(vinylcyclohexane) (PVCH) has been investigated by electron diffraction and dark-field imaging following a procedure introduced by Pradère et al. (*Macromolecules* **1988**, *21*, 2747). Crystals produced in thin film at high T_c are single crystalline. At somewhat lower T_c, they display large twinned sectors bounded by (200) and (020) planes only. PVCH crystals produced from squalane or phenyldecane solutions display very small, elongated twinned domains oriented normal to the growth faces: the crystals are made of polysynthetic twinned growth sectors. A specific and growth sector dependent streaking indicates that the lattices are shifted by one-quarter of the unit-cell edge across the twin planes: the growth faces are jagged. These features are discussed in the general context of polymer nucleation and growth. Deposition of the initial stem in the growth face takes advantage of the existing step associated with the twin plane, a process that can be described as a "fractional" secondary surface nucleation process. Lateral spread, i.e., completion of the growth face, is limited by the jagged surface. Since both secondary nucleation and lateral spread are determined or limited by structural features, the usual distinction of different growth regimes is blurred.

Introduction

The internal structure of polymer single crystals is most easily investigated by electron diffraction and dark-field imaging. The latter technique, in particular, indicates that different growth sectors may diffract differently depending on the orientation of folds or on the existence of corrugations or pleats.[1] Dark-field imaging has also been used to reveal twin planes and twinned sectors in, among others, simple or multiple twins of poly(ethylene oxide)[2] and polyethylene.[3] In the present contribution, we use extensively dark field imaging to reveal the internal structure of single crystals of isotactic poly(vinylcyclohexane) (PVCH). More specifically, we observe that the crystals may be polysynthetic twins—a rare case in polymer science, that has however wider implications. For this purpose, we use a dark field imaging technique pioneered by Pradère et al.[4]

Pradère et al. have used dark-field imaging to show that single crystals of isotactic poly(4-methyl-1-pentene) (P4MP1) in its crystal modification III display frequently twinned domains that are generated as a result of growth twinning. Their observations were made possible by the fact that modification III of P4MP1 has a tetragonal unit cell with $I4_1/a$ symmetry, as shown by De Rosa et al. in a later structure determination of this form.[5] The 4-fold helices are tilted relative to the *a* and *b* axes. As a result, the diffraction pattern "has a sense": the intensity of some *hk*0 reflections may differ significantly from that of the corresponding $\bar{h}k0$ or $kh0$ reflections (e.g. 240 versus $\bar{2}40$ or 420), depending on the clock- or anticlockwise rotation of the helices on their axis relative to the cell edges. When twinned domains coexist in a single crystal, the corresponding *hk*0 and *kh*0 reflections overlap (as is usually the case in twins by merohedry) and it is not normally possible to suspect the existence of twinned sectors. Pradère et al. were nevertheless alerted by curious variations in the relative intensities of these critical, overlapping reflections. Dark-field imaging made it possible to differentiate those parts of the single crystal that diffract more or that diffract less, i.e., allows a mapping of the twinned domains. Pradère et al. showed that the single crystals of form III of P4MP1 are made of relatively large domains in twin relationship, with (200) or (020) and (110) twin planes. To our knowledge, this elegant use of electron diffraction and dark-field imaging pioneered by Pradère et al. has not been pursued in later work. It has, however, the potential to become a powerful investigation tool that gives access to features of the structure of polymer single crystals (and more generally polymer lamellae) that are not accessible by any other investigation technique.

In the present paper, we investigate single crystals of a high-melting (>400 °C) polyolefin, isotactic poly(vinylcyclohexane) in its form I, a crystal modification that also has $I4_1/a$ symmetry.[6] Combining dark-field imaging with the analysis of specific streaks in the diffraction pattern makes it possible to show that, for certain crystallization conditions, growth sectors are actually polysynthetic twins. As a result of this twinning, the crystals are bounded by nonplanar, molecularly jagged growth fronts. This observation is discussed in the context of nucleation and growth processes. It suggests that the deposition of a crystalline stem on a flat surface (secondary nucleation) usually considered can be supplanted by a different nucleation that takes advantage of the crystallographic shifts associated with these twin planes. The favored deposition sites are the twin planes abutting on the growth face. This initial deposition step (secondary nucleation) has some of the features of the lateral spread, which introduces the unexpected concept of "noninteger" or "fractional" secondary nucleation processes in polymer science. Its impact in crystal growth of other polymers and in spherulitic crystallization is discussed.

* Corresponding author. E-mail: lotz@ics.u-strasbg.fr.
[†] CNRS-ULP.
[‡] Present address: Institute of Materials Science and Engineering, National Sun Yat-sen University, Kaohsiung 804, Taiwan.
[§] Ritsumeikan University.

10.1021/ma0523217 CCC: $33.50
Published on Web 12/20/2005

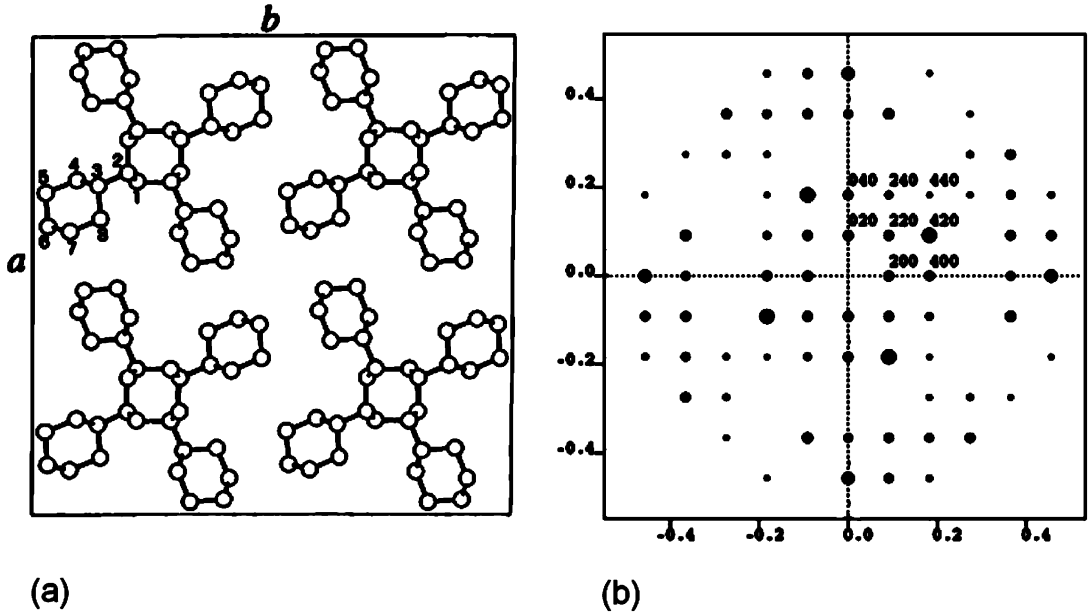

Figure 1. **(a)** Crystal structure of PVCH in *c* axis projection, as determined by De Rosa et al.[6] **(b)** *hk*0 diffraction pattern of PVCH, as computed with the Cerius[2] modeling package.

Experimental Section

Sample and Preparation Methods. The sample of PVCH was the same as that used in a previous study by one of the authors.[7] It was provided by Sumitomo Chemical Co. Ltd. Its molecular weight is about 2.4×10^5.

The preparation of suitable single crystals was based on three different procedures: from solution, from the melt, and by a less standard "solution-assisted melt crystallization". As is classical with high-melting polymers, solution crystallization was performed from a squalane solution (bp $\approx$ 350 °C). Solution-grown crystals were directly deposited on carbon-coated electron microscope grids. An alternative suitable solvent was phenyldecane, with a lower bp (115 °C). To investigate melt crystallization, thin films were produced on a hot bench, by slow evaporation (sliding back and forth) of a drop of the polymer solution beneath a razor blade mount. However, this procedure turned out to be partially inappropriate. Indeed, maintaining the sample at high temperature for long periods inevitably resulted in some dewetting of the polymer melt. As a result, the thickness of the film became excessive for transmission electron microscopy. We were thus led to devise a "composite" operational mode by which the solution is inserted between two glass cover slides or mica sheets. The sandwich cover slides are mounted on the heating stage of an optical microscope and heated under a nitrogen flux. Evaporation of the solvent under these conditions results in a less uniform film thickness that was found appropriate: whereas many areas are still too thick, this procedure also generates relatively large domains with reasonably dense populations of monolamellar crystals highly suited for our investigation.

As a rule, slow cooling has been used. For thin films, the cooling rates could be controlled in the hot stages. For solution crystallization, and especially for squalane, the heating of the oil bath was disconnected and the bath allowed to cool to room temperature. This corresponds to cooling rates of $\approx$0.4 °C/min in the crystallization range. The thermal treatments were carried out in Mettler FP 80 or Linkam 600 hot stages, under a nitrogen blanket, and growth could be followed in situ.

The samples are shadowed with Pt when desired and coated with a carbon film. Detachment of the crystals from the glass support is rendered difficult by the extended stay at high temperature: the polymer tends to stick to the glass slide. When the usual detachment with a poly(acrylic acid) backing did not work, partial dissolution of the glass support slides by hydrofluorhydric acid was used.

Techniques. Observation of the crystal morphology was performed under phase contrast with Leitz and Zeiss optical microscopes. Electron microscopic examination was performed with a Philips CM12 instrument operated at 120 kV. Bright-field images, diffraction patterns, and dark fields were recorded with an Imagix MegaView III digital camera (Soft Imaging System) and/or on photographic plates (Kodak SO163, developed with undiluted D11 for 12 min). To limit the impact of electron beam damage, the crystals are examined at low magnification using the defocused diffraction pattern mode. Given the acceptable lifetime of this polymer under the electron beam, one dark-field (which is sufficient for a full structural analysis) and sometimes two dark-field images could be recorded on photographic plates at a direct magnification of 3000.

Molecular modeling and analysis of the diffraction patterns were performed with the Cerius[2] package of Accelrys. The Diffraction Faulted module was used to model the streaking of the diffraction patterns.

Results and Analysis

Background: Polymorphism of PVCH and Asymmetry of Form I. PVCH is a polyolefin that bears a bulky, ramified lateral group: the cyclohexyl ring corresponds indeed to a substitution in the α position of the side chain. As for most polyolefins with a ramification next to the main chain, it has a high melting temperature (>400 °C). Two chain conformations have been observed for PVCH: a 4-fold helix (the stable crystal modification under investigation in the present study) and a crystal modification obtained only upon drawing at high temperature, with a helix geometry including 24 residues in 7 turns (i.e. nearly 3.5 residues/turn). The two crystal modifications interconvert into each other: form I into form II by drawing at high temperature (>130 °C); form II into form I by heating at $T >$ 238 °C.[7]

The unit-cell geometry of the stable crystal structure is tetragonal with parameters $a = b =$ 21.99 Å and $c =$ 6.43 Å. The unit-cell symmetry—the space group—is an important ingredient in the present analysis. De Rosa et al. determined it to be $I4_1/a$.[6] This implies that the cell contains four (isoclined) helices, two right-handed and two left-handed helices. Furthermore, in this space group, the azimuthal setting of the helices is such that the projections of the 4-fold helices are not parallel to the cell edges (Figure 1a). As a consequence, the diffraction pattern displays a polarity. When considering the set of strong

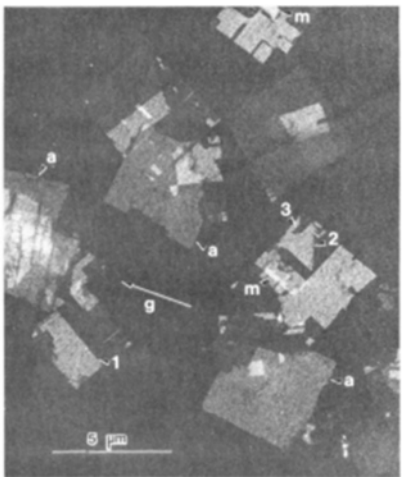

Figure 2. Single crystals of P4MP1 produced by Pradère et al.[4] and imaged by dark-field imaging through the overlapped (240, 420) reflection. Note the formation of growth twins at various stages of the crystal development, and the existence of both (200) (and equivalent (020)) twin planes as well as (110) twin planes.

reflections indexed as 020, 220, and 420 and the corresponding reflections with negative indexes, they form a pattern of arms that rotate clockwise in Figure 1b. Since the helix azimuthal orientation relative to the cell edges determines the relative strength of the 240 and 420 reflections, this azimuthal setting is indicated by the "sense" of the diffraction pattern: clockwise or anticlockwise. The diffraction pattern thus provides an easy and immediate means to determine the sense of the azimuthal setting of the helices in the unit cell. It is also clear that this azimuthal setting depends on the sense of observation of the crystal: when examining a given crystal but oriented upside down in the electron microscope, the azimuthal setting changes. In the case of the isotactic poly(4-methyl-1-pentene) form III mentioned in the Introduction, this led Pradère et al. to suggest that the composite crystals might be made of domains that differ by the up or down orientation of their helices, whereas also discussing (correctly) their observations in terms of twinning.[4]

As a further comparison of results to be presented shortly and the earlier work on single crystals of P4MP1 form III, we show in Figure 2 one image published by Pradère et al.[4] It represents a dark field obtained from solution-grown single crystals using one combined (240, 420) diffraction spot. The crystal is made of domains in which the helices have different azimuthal settings. As a result, domains imaged with the strong 420 diffraction spot appear as bright, whereas domains imaged with the weak 240 spots are significantly darker. For future reference, note that, for these P4MP1 form III crystals, the twin boundaries are parallel to either (200) or (020) planes, as well as (110) planes. The (110) twin planes are not necessarily associated with growth sector boundaries. Growth twins seem to be the rule: new twinned domains are generated as a result of the deposition of a new layer in twinned orientation relative to the substrate, virtually at any stage of the crystal's growth and in any location on that crystal's edges.

Diffraction and Dark-Field Imaging of Single Crystals of PVCH Form I. The morphology and structure of the PVCH single crystals depend very significantly on the preparation method.

In thin films crystallized at high temperature, the crystals frequently have a four-leaves cloverleaf morphology (Figure 3a). These single crystals yield a simple, "untwinned" diffraction pattern, with strong 240 and weak 420 spots (Figure 3b). The chains are oriented parallel to the electron beam, i.e., normal

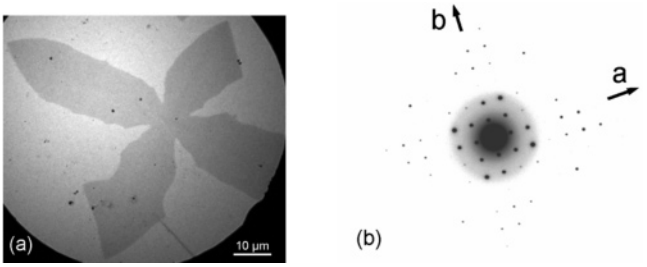

Figure 3. **(a)** Single crystal of PVCH produced at high temperature. The four arms of the crystal are elongated along the ⟨110⟩ direction. **(**b**)** Associated diffraction pattern. The asymmetry of the pattern (compare 240 and 420 reflections and cf. Figure 1b) confirms the cell symmetry determined by De Rosa et al.[6] and indicates that the crystal is untwinned.

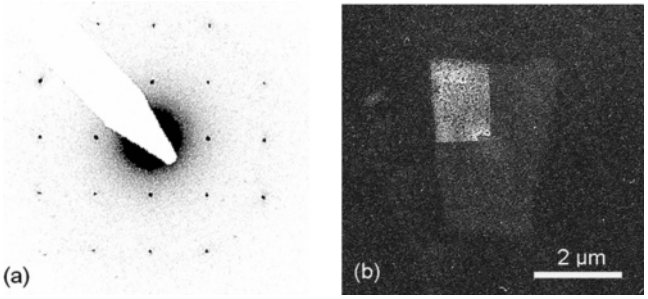

Figure 4. **(a)** Diffraction pattern and **(**b**)** corresponding dark field of a crystal of PVCH from the melt. The dark field (imaged through 420 or 240 reflections) displays large twinned domains. In all PVCH square crystals shown in this and subsequent figures, the *a* and *b* axes are normal to the growth faces.

to the lamellar surface. Dark-field images of the crystals (not shown) are rather dull and un-informative: their uniformity (to be contrasted with later images) confirms that the crystals are essentially untwinned. The fastest growth direction of the arms of the clover leafs is parallel to the ⟨110⟩ directions. The arms are bounded occasionally by (200) or (020) planes, but more generally the edges are rounded and it is difficult to point out any given preferred growth plane.

A majority of single crystals produced from thin films are more complex (Figure 4). Their diffraction pattern displays the different relative intensities of 240 and $\bar{2}40$ or 420 reflections that had alerted Pradère et al. in their investigation of P4MP1 form III single crystals. Indeed, the dark-field images reveal that the crystals are made of a variable number of relatively large sectors in twin relationship. Any one crystal may either be single crystalline or contain as little as two twinned sectors, but the number of these sectors can be more important. Compared to the P4MP1 form III crystals investigated by Pradère et al. (cf. Figure 2), the boundaries of the twinned sectors in PVCH are always parallel to (200) and (020) faces, with no (110) twin boundaries.

The most original twinned features have been observed in single crystals produced from PVCH solutions in squalane and phenyldecane. In both cases, the thermal history was not adjusted to e.g. control the concentration of seeds by the self-nucleation technique, in view of the high dissolution/melting temperatures involved. Crystals in the ≈10 μm range or even bigger could be obtained, which were mandatory to obtain sufficiently detailed dark-field images.

Crystals produced from dilute solution in squalane display diffraction patterns in which the reflections indicative of twinning have equal intensity, suggesting that the two twinned crystal orientations exist in equal proportions (Figure 5a). Furthermore, the diffraction patterns display one feature that

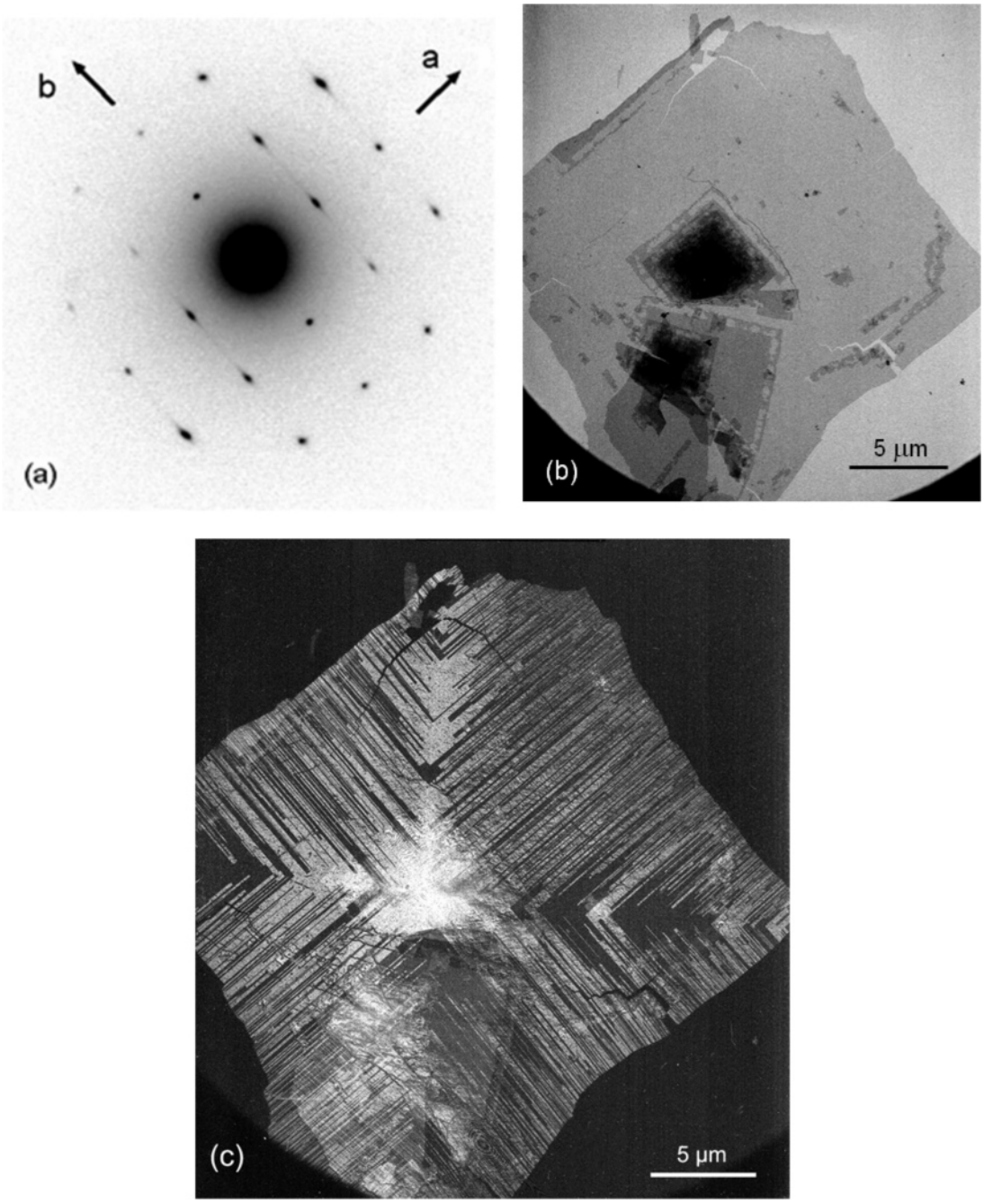

Figure 5. Crystals of PVCH formed in a squalane solution. The polymer was dissolved in boiling squalane (350 °C), the solution was taken to 220 °C and slowly cooled. **(**a**)** Electron diffraction pattern taken from the upper right growth sector in part b. Note that the critical reflections 420 and 240 have equal intensity, indicating that the twinned domains coexist in equal proportions in the crystal, as a result of the multiple microtwinning (compare with Figure 3b). Note also the streaking of some reflections, best revealed here by a logarithmic representation of the intensities. **(**b**)** Corresponding bright field. Note the existence of the central screw dislocation and crystal debris. **(**c**)** Dark-field image obtained through one set of overlapped 420_I and 240_{II} reflections of twinned domains I and II that differ by the azimuthal setting of the helices. The bright domains are imaged through the strong 420_I reflection; the dark domains, through the overlapped but weaker 240_{II}. A similar dark field (not shown) but with poorer quality (as a result of electron beam damage) is obtained when using the overlapped weak 240_I and strong 420_{II} reflections. The bright and dark domains are simply inverted. A single dark-field image is thus sufficient to map the distribution of twinned domains.

had not been observed so far, both in the P4MP1 crystals of Pradère et al.[4] and in the PVCH crystals produced in thin films (Figures 3 and 4): *some reflections are streaked*. More specifically, the streaking *is growth sector dependent*. For any given growth sector, the (say) 200 and 2*h*20 reflections are streaked, whereas the 020, 040, and (most importantly) the 400 reflections are not streaked. Moreover, the streaking extends in a direction that is parallel to the growth front of the selected growth sector. This streaking indicates a structural disorder that is repeated at a much smaller scale than in single crystals produced in thin films. It should be noted that this streaking might have escaped us had we not had the possibility to display the intensities of the diffraction pattern on a logarithmic scale. The pattern shown in Figure 5a takes advantage of this possibility.

Dark-field imaging using the critical 240 or 420 spots confirms the existence of a significant structural disorder (Figure 5c). It reveals that the "single crystal" is actually made of a complex pattern of elongated twinned microsectors, oriented systematically perpendicular to the growth face and bounded by (200) or (020) twin boundaries. In the growth direction, the microsectors are very long, sometimes extending from the crystal

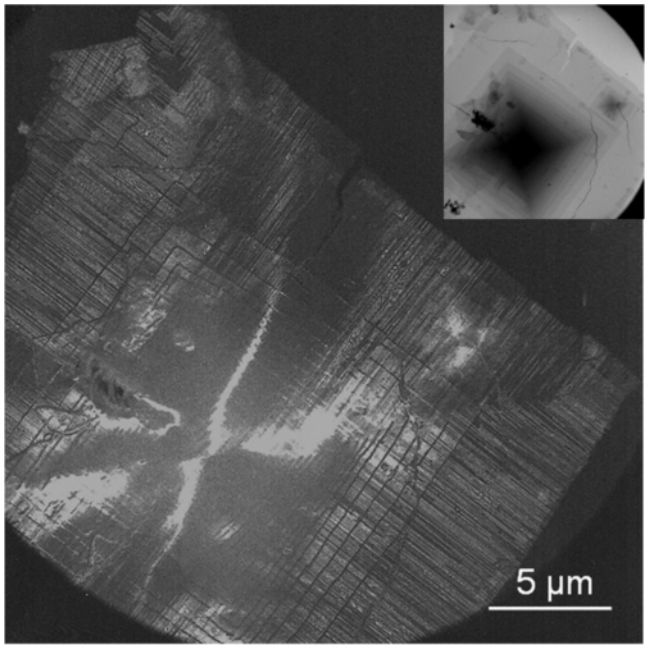

Figure 6. Bright- (inset) and dark-field imaging of a crystal of PCVH grown in a squalane solution and displaying a central screw dislocation. The large lamella is imaged by dark field although it is covered by other lamellae.

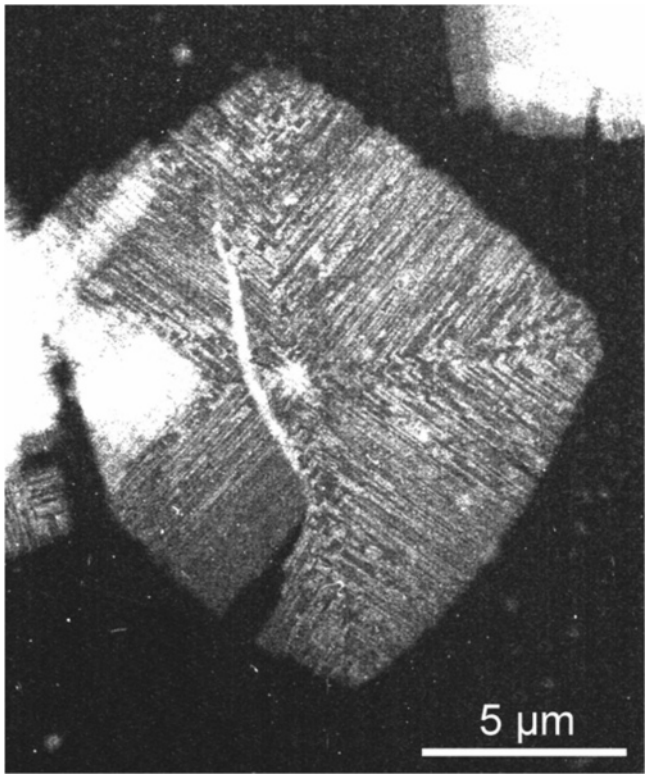

Figure 7. Single crystals of PVCH produced in a phenyldecane solution and observed in dark field imaging mode. Although the general organization in elongated twinned domains prevails, the twinned domains are shorter, i.e., frequently interrupted by a new growth twin that restores the initial stem orientation. Contrast digitally enhanced to better visualize the differences between microdomains.

center or growth sector boundaries to the outer edges of the crystal. This feature suggests that the depositing helix "feels" and reproduces the azimuthal setting of the underlying helix in the newly formed layer. Laterally, the dimensions are remarkably small, down to 10 nm or a few tens of nanometers, but some twinned domains extend up to hundreds of nanometers.

A technical detail is worth emphasizing, as best illustrated in the dark-field images obtained from a screw dislocation, shown in Figure 6. Since the dark-field images use a reflection that is specific to one lamella only (the largest one in this case), the structure of the whole lamella can be analyzed, although this lamella is covered by additional lamellae arising from a screw dislocation or by occasional debris of other single crystals (cf. the bright fields in Figure 5b and Figure 6, insert). Thanks to this imaging technique, mapping of the twinned microdomains is possible over the whole crystal surface, including those parts that in bright field are "hidden" by overlapping crystals. One may further note that when crystals overlap the crystal of interest, occasional moiré patterns appear in the dark-field image (perhaps lost in print).

The crystals formed in phenyldecane display essentially the same features—with some interesting variations in their details. The crystals are overall rounded squares, the rounding being possibly a reflection of their original "bowllike" shape, to use the wording of Khoury and Barnes.[8] Indeed, the crystals display some pleats oriented nearly normal to the crystal sector boundaries. These pleats arise when an initially nonplanar, bowllike crystal collapses on a flat surface. More relevant to the present topic, the crystals yield again sector-dependent streaked diffraction patterns. Dark-field imaging reveals also a complex structure with twinned microsectors (Figure 7). These sectors, although elongated in a direction normal to the growth front, are frequently shorter than for crystals produced in squalane. This suggests that repeated growth twins develop relatively easily on the growth front, which results in more frequent alternation of the azimuthal orientations.

Multiple, narrow twinned domains with parallel twin boundaries define the solution-grown single crystals of PVCH as "polysynthetic twins". Polysynthetic twins are well-known in the field of mineralogy (e.g. for layered silicates), but to our knowledge they have not yet been observed or reported in the field of polymer single crystals. As examined next, they happen to provide unusual insights in the detail of the twin planes organization, in nucleation and growth mechanisms of this polymer—and also, possibly, of crystalline polymers in general.

Streaked *hk*0 Diffraction Patterns and the Organization of Helical Stems in the Twin Plane. The detailed packing mode across a twin plane is usually difficult to analyze. Indeed, we are dealing with a local defect (or a row of local defects) that does not leave much trace in, for example, the diffraction pattern. Direct imaging of the twin plane by high-resolution electron microscopy is of course possible for metals or minerals, but is usually precluded for polymers due to their beam sensitivity (with some exceptions, as examined soon). As a consequence, detailed knowledge of the twin planes is usually lacking, although twins in polymers have been investigated extensively.

Investigation of polysynthetic twins in PVCH single crystals provides an unusual opportunity to investigate the details of the twin plane structure. Indeed, because the structural disorder associated with twinning is repeated on a small scale, it results in the formation of streaks in the diffraction pattern (Figure 5a). No streaks would be observed if the density of twin planes were much reduced.

The structural disorder associated with the twin planes can be easily determined from the characteristics of the streaked pattern, and more specifically from the reflections that are, or are not, streaked. In the pattern displayed in Figure 5a, the 200, 220, and 420 reflections are streaked, whereas the 020, 040, and 400 reflections are not streaked. Absence of streaking indicates that the structural disorder is not "seen" by the

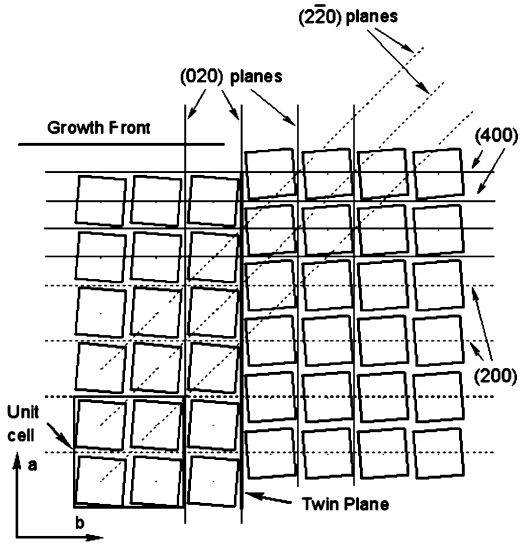

Figure 8. Origin of the streaks in the diffraction pattern of polysynthetic twinned crystals. The features of the streaking indicate that a shift of a quarter of a cell edge of the crystal lattice across the twin plane is involved. Diffraction spots that are not streaked correspond to the planes shown in full lines, whereas streaked spots correspond to planes shown in dotted lines. Only for the latter are the fractional coordinates of the helices affected by the twin plane.

crystallographic planes considered. The fact that 020 and 040 are not streaked indicates that the twin plane is oriented parallel to the *a* axis and that layers of helices parallel to the *a* axis are linked by a mere reflection parallel to these planes. The fact that 200 is streaked but 400 is not indicates that the layers just considered are shifted by one-quarter of the unit-cell edge along *a* (Figure 8).

The above analysis can be complemented and supported by a modeling of the structural disorder, using the "Diffraction Faulted" module of the Cerius[2] package. The module stacks different crystalline layers with adjustable probabilities of packing and calculates the diffraction pattern either as a selected area diffraction pattern (SADP) or as a profile of intensities along selected layer lines. The two models used in the modeling are represented by the two top layers in Figure 10 (cf. later), in relative position across the twin plane. Parts a−d of Figure 9 display the SADP and the intensity profiles along layer lines 0*k*0, 2*k*0, and 4*k*0, respectively. The layers and therefore the twin planes are parallel to the *a* axis; the stacking probabilities have been set at 0.9 to maintain the same layer and 0.1 to change the layer type, i.e., to generate a twin plane. The resulting single crystalline strips thus are ≈10 nm wide on average (which is a realistic figure for the narrowest twinned domains). Unstreaked reflections are, as expected, located on the symmetry axes of the SADP: along *a** (400), along *b** (020 and 040), and on the diagonals of the pattern (440). However, as expected also, all reflections on the layer line $h = 2$ (including 220) are streaked, since the structural disorder affects these planes most.

As far as the *packing scheme* of helices across the twin plane is concerned, the *a*/4 (or *b*/4) shift of helices in PVCH is most plausible. The essential ingredients of the reasoning are summarized in Figure 10, considering only *c* axis projections of the structure. Due to the azimuthal tilt of the helices in the unit cell, a pure reflection twin appears rather unlikely: indeed, the facing helices across the twin boundary have opposite azimuthal settings, which generates a succession of "empty" wedges along the twin boundary (bottom twin plane). However, by shifting along the twin plane one component of the twin by one-quarter of the unit-cell edge (i.e. by half the lateral span of one helix),

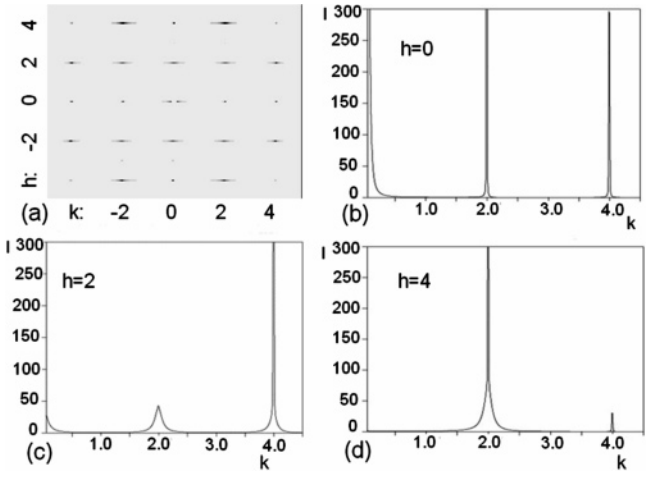

Figure 9. Modeling of the streaked diffraction pattern of PVCH single crystals using the Cerius[2] "Diffraction Faulted" module. The top two layers shown on top of Figure 10 are stacked with a 90% chance to maintain the same layer and 10% to generate a twin plane. **(a)** Modeling of the selected area diffraction pattern; **(**b−d**)** intensity profiles along the layer lines indicated.

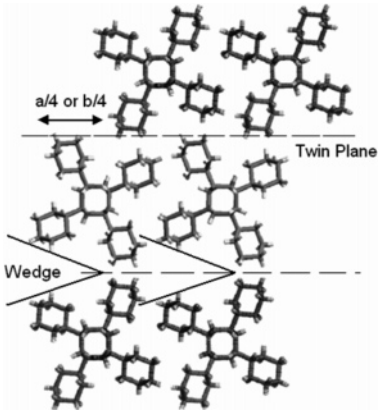

Figure 10. Packing of 4-fold helices across two possible (100) twin planes. A pure reflection twin (lower part) generates a succession of empty wedges. Shifting of the twinned layer by half a helix width removes part of these empty wedges (upper part). The latter situation prevails in PVCH.

these wedges disappear since the bulges of one plane fit in the troughs of the facing plane (top twin plane). Best packing across the twin plane is achieved when two features add up: reflection across, and shift by one-quarter of the unit cell along, the twin plane.

Streaked diffraction patterns are not uncommon in polymer science and have been observed for many polymer single crystals that display a structural disorder (but not necessarily associated with twinning or microtwinning). It has been analyzed for single crystals of syndiotactic polypropylene (sPP).[9] Also, similar streaked patterns, analyzed as arising from different stacking of layers ("stacking faults"), have been reported for crystals of the orthorhombic β modification of syndiotactic polystyrene (sPS).[10] In this case, dark-field imaging is less informative since the domains are very narrow (down to two layers, i.e., one unit-cell edge).[11] Resorting to high-resolution electron microscopy at liquid helium temperature helped reveal the organization of the chains within the βsPS single crystals and at the stacking faults: reflection and translation of layers are also involved in βsPS.[11]

Formation and Preservation of the Twin Planes during Crystal Growth. Due to the tetragonal symmetry of the PVCH unit-cell, twin planes can be oriented parallel to the *a* axis and/

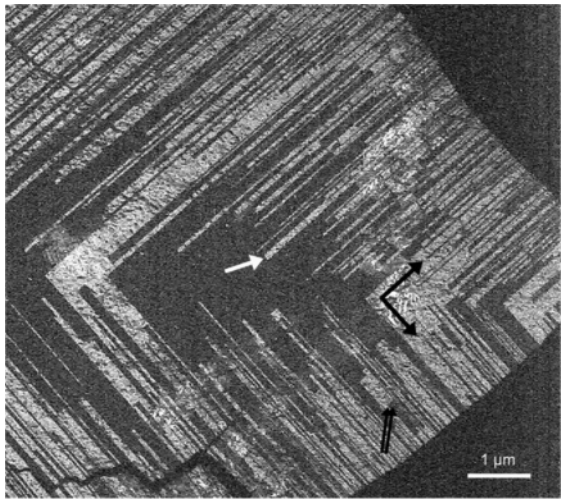

Figure 11. Enlargement of the dark-field image of a PVCH crystal with microtwinned sectors (Figure 5c) illustrating the appearance and disappearance of twinned microsectors as a result of growth twinning (arrowed). Newly formed domains have edges parallel to the growth front, indicating the extent of lateral spread through secondary nucleation. Bright and dark domains extend over (110) growth sector boundaries, indicating that the helix orientation is preserved.

or the *b* axis, that is, either parallel or normal to the growth front in any one growth sector. It is therefore of interest to examine—with the help of the dark-field images—what twinning takes precedence in the generation and preservation of the twinned microsectors. An enlargement of a dark field is shown in Figure 11 to illustrate the argument.

The initial limit (that is, the inner limit) of a twinned microsector is, as a rule, oriented parallel to the growth front (cf. arrowed boundary in Figure 11). Nucleation of the twinned microsector can thus be considered as a conventional secondary nucleation process in which, however, the initial stem is located halfway between the two substrate helices (rather than in front of them, as required by the crystal symmetry) and with its azimuthal setting in twinned relationship to the substrate ones (cf. later, helix marked 5 in Figure 12b). This twinned orientation spreads on the growth face and is limited by its encounter with parts of the layer that have grown from other nuclei. In other words, the dimensions of these (ultimately) microdomains gives a (rough) estimate of the lateral spread under the crystallization conditions prevailing in the squalane or phenyldecane solutions. Our dark-field images (cf. Figure 11) indicate lateral spreads ranging from 30 to 150 nm (the same number of stems).

Further support for a secondary nucleation-type mechanism with twinned orientation of the depositing helix is provided by the fact that some twinned microsectors "revert back" to the initial orientation of the helices with, again, a boundary parallel to the growth front and a lateral spread that may vary: indeed, whole (or parts of) twinned microsectors "terminate" at different stages of the crystal growth (cf. double arrow in Figure 11). It appears therefore that generation (and, as just discussed, annihilation) of twinned microsectors can be safely analyzed as a classical example of growth twinning.

The mechanisms by which the twinned microsectors are perpetuated during growth are more original and at the same time more complex.

The initial nucleation process just described generates twinned domains with the twin plane and associated shift of helices parallel to the growth front. However, the dark-field images indicate that the major twin planes are perpendicular rather than parallel to the growth front. Also, the streaked diffraction pattern indicates that the associated shift of helices is perpendicular to the growth front. This observation indicates that the twinned components, shifted initially parallel to the growth front (say, along the *b* axis when the growth planes are (200)), must also become shifted parallel to the *a* axis through the agency of local defects. The details of this process are difficult to analyze, but once this shift is generated, it is perpetuated during further growth, usually up to the outer crystal edge. We will refer to these twin planes perpendicular to the growth front as "twinned sector boundaries".

The above analysis thus indicates that we are dealing with two related but different manifestations of twinning in PVCH crystals: by deposition on the growth front, which generates "local" growth twins with boundaries parallel to the growth front (these growth twin boundaries are not very numerous and are of limited lateral extension) and twinned sector boundaries normal to the growth front that perpetuate the (sometimes very narrow) twinned domains generated by the twinned secondary nucleation process. The latter twin boundaries act as an amplifier that helps visualize the formation of growth twins. Since more and more such growth twins are formed during growth, the density of boundaries that limit twinned growth sectors tends to increase from the crystal center to the crystal edges—probably with some upper limit.

The mechanisms by which these twinned sector boundaries normal to the growth front are preserved during growth are analyzed in Discussion. For the present, we note that the structure of the twin planes is also consistent with the fact that only (200) and (020) twins are observed in the crystals of PVCH. Indeed, the *a*/4 (or *b*/4) shift of helices precludes development of (110) twin boundaries. The latter would correspond to a line of structural defects of high energy, since the shifts in the two twinned components would be at right angles to each other. Note however that the growth sector boundaries in the single crystals are parallel to the (110) planes of the tetragonal PVCH unit cell. For most of the microtwinned sectors, crystallographic continuity is almost systematically maintained across these (110) growth sector boundaries (cf. Figure 11, black arrows at right angle). The dark and the bright domains "take the corner" at the sector boundaries, which means that the helices maintain their azimuthal setting, and no twin plane is associated with these growth sector boundaries.

Discussion

The structural analysis of PVCH crystals grown from solution reveals a complex pattern of twinned domains. The structure of the twinned domain boundaries has been established, thanks to the streaking of the diffraction patterns. These analyses indicate that the topography of the growth faces is more complex than for untwinned crystals, which has necessarily an impact on the nucleation and growth of these crystals. This discussion section is mainly concerned with secondary nucleation and completion of the growth faces by lateral spread. It introduces the concept of "fractional" secondary nucleation, a nucleation process that takes place at the twin plane when the latter generates a jag on the growth front. It further considers the major differences between the impact of a single and of multiple twin planes (as observed in PVCH) on the growth kinetics of single crystals and, tentatively, of more complex morphologies (spherulites).

Impact of the Twin Planes on Nucleation and Growth of PVCH Crystals. One major conclusion can be drawn from the above analysis of the streaked diffraction pattern of PVCH crystals: the crystal parts that are in twin relationship are shifted

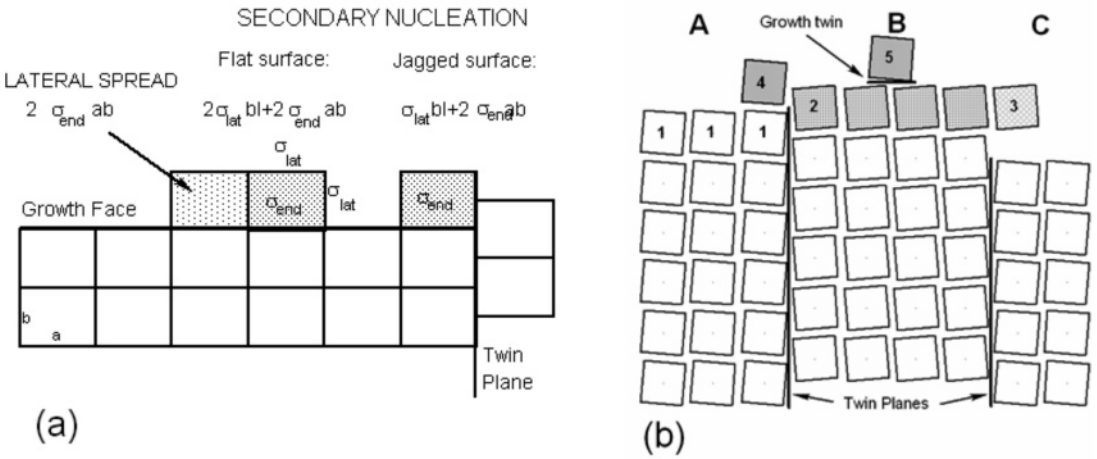

Figure 12. (a) Comparison of energy balances for secondary nucleation taking place on a flat growth face, for "fractional secondary" nucleation next to a twin boundary (dark shading) and for the lateral spread along (completion of) the growth face (light shading). (b) Schematic representation of the various nucleation processes that can take place at and near the twin planes abutting on a growth face. Three twinned domains are represented, with domain A in front of domain B and C. Domain A (helices marked 1) is the initial crystal growth face. The most favorable nucleation site is at position 2 ("fractional" secondary nucleation). Completion of the growth face of domain B (shaded helices) stops at the next twin boundary: deposition of helix 3 corresponds to a true "secondary" nucleation step. Rather, the twinned domains grow via further fractional secondary nucleation (e.g. helix marked 4). New growth twin planes may be generated by conventional deposition (secondary nucleation) in twin relationship with the substrate growth faces (helix marked 5).

by one-quarter of a unit cell, or by half the span of a helix in the unit cell. As a result, when twin planes abut at right angles on growth faces, the latter are molecularly *jagged*. We examine now how the existence of such local defect(s) is likely to affect the growth of the PCVH crystals.

We first recall the essential features of crystal growth. In the classical nucleation and growth scheme, growth of single crystals is considered to take place via secondary nucleation.[12] The secondary nucleation consists of the deposition of a new stem on a *flat* surface, followed by the filling in of the new layer by lateral accretion of successive stems next to the last deposited stem (Figure 12a). Energetically, the secondary nucleation is more costly, since it necessitates the formation of two new lateral solid/melt interfaces in addition to the two end surfaces. Lateral spread necessitates no formation of lateral surfaces, only of the two end surfaces. The energy barriers to overcome are thus

$$\text{secondary nucleation: } 2\sigma_{end}ab + 2\sigma_{lat}bl$$

$$\text{lateral spread: } 2\sigma_{end}ab$$

where σ_{lat} and σ_{end} represent the lateral and end surface energies and a, b, and l the stem width, thickness, and length, respectively.

Also, in the so-called regime I, secondary nucleation is the rate-determining step since it is much slower than completion of the layer by lateral spread. In regime II, a higher density of secondary nucleation steps limits the lateral spread along the growth face.

The existence of a jagged surface is likely to affect both the nucleation and the growth processes (Figure 12b).

We consider the secondary nucleation process first. Deposition of the first stem is likely to take place at the twin boundary rather than on a flat surface. Indeed, one microsector is ahead or behind its twinned neighbor by one-quarter of a unit cell, or half the stem thickness (≈5 Å in PVCH). Nucleation is thus favored at the twin boundary (chain marked 2 in Figure 12b). Deposition of a new chain creates less new lateral interfacial energy ($0.5bl\sigma_{lat}$) and takes advantage of the extra lateral free energy linked with the local protrusion or "overhang" of the growth front ($0.5bl\sigma_{lat,twin}$). It is further reasonable to assume that $\sigma_{lat,twin} \approx \sigma_{lat}$, given the high frequency of growth twins in PVCH. The energy balance associated with the deposition of a stem at the twin boundary is thus (Figure 12a):

$$\text{secondary nucleation at a twin boundary: } 2\sigma_{end}ab + \sigma_{lat}bl$$

The impact of lateral spread is equally affected, in particular for the crystals that display short-range, polysynthetic twinning (cf. again Figure 12b). Indeed, lateral completion of the growth face takes place on the available substrate length. For a jagged growth face, however, lateral growth can extend only up to the next twin boundary. At this point, the growth front of the next twinned microsector is (say) lagging behind (domain C). Deposition of a chain in the direct continuation of the layer just deposited would correspond to a true secondary nucleation process and is therefore much less probable (chain marked 3). To the contrary, in this simplified scenario, the next microsector will resume growth, starting at the twin plane, since it allows now for a less costly *"fractional secondary"* nucleation step.

To summarize, the existence of these multiple twin boundaries modifies significantly the nucleation and growth processes in both the "academic" situation of the so-called regime I growth and even in regime II for a high density of twin planes. In essence, the secondary nucleation step (deposition of a new stem on a flat substrate growth layer with generation of a lateral surface energy equal to $2bl\sigma_{lat}$) is replaced by a fractional secondary nucleation step in which less lateral surface is created, and a further fraction of the lateral energy is compensated for by the interaction with the protruding helix of the neighbor twinned domain. As a result, the lateral surface energy that needs to be overcome is halved: it is only $bl\sigma_{lat}$. In both cases, the lateral spread is similar. However, the impact of lateral spread on the growth rate is limited by the width (breadth on the growth front) of the microtwinned domains, namely, by a structural feature.

Simple and Multiple Twins in Polymer Single Crystals. Twinning in polymer crystals or single crystals is by no means a new feature. Twins have been investigated from the very early days of this field, with forerunners Khoury and Padden, who investigated single crystals of polyethylene.[13] Twins and multiple

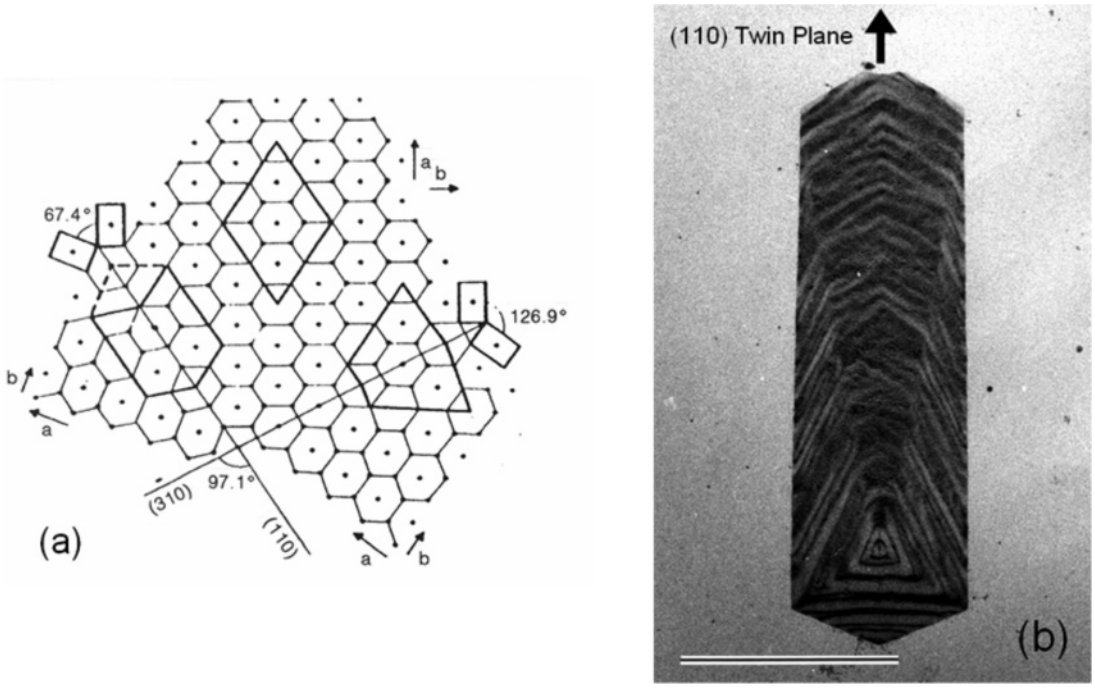

Figure 13. **(**a**)** Illustration of the polyethylene crystal lattice, the untwinned crystal, the (310) twin, and the (110) twinned crystal with its acute angle at the (110) twin boundary. The PE lattice is represented here as (pseudo)hexagonal rather than orthorhombic. **(**b**)** (110) twinned crystal, illustrating the faster growth along the (110) twin plane. Parts a and b: Reprinted with permission from ref 3. Copyright 1993 VCH.

twins of poly(ethylene oxide) (PEO) and of polyethylene (PE) single crystals were described in extensive detail by Kovacs et al.[2] and by Wittmann and Kovacs,[3] respectively. For PE, different twin plane structures have been considered by Burbank.[14] An analysis of packing in twin planes (and orthorhombic to monoclinic phase change) is due to Geil et al.[15] For PEO, a systematic and exhaustive classification of "single crystal" multiple twins based on the combination of two twin modes could even be proposed.[2] Several of these examples will be used in later parts of the discussion.

Considering only growth twins of interest in the present context (as opposed to mechanical twins), we note that the twin planes may have different origins. In the PEO and PE examples considered above, the crystal nuclei are twinned (in the case of PEO by deliberately using a quench-self-seeding procedure).[2] Later crystal growth simply acts as a magnifying lens to reveal the twinned nature of the single crystals' seeds: no new twin planes are formed during the growth stage.

The complex twins of P4MP1 form III investigated by Pradère et al.[4] are growth twins and are, as in PVCH, formed during the later stages of growth. Initially untwinned crystals may become twinned as a result of this process. Furthermore, the twin planes are oriented both parallel and normal to the major growth faces of the single crystals (for *h*00 or 0*k*0 twin planes) or oblique for the (110) twin planes in P4MP1 form III.

The structure of the twin boundary is not known in any detail for most polymers investigated so far. We reproduce in Figure 13a the drawings of Wittmann and Kovacs that illustrate (110) and (310) twins of PE[3] and a similar, updated drawing for the PEO twins (Figure 14a).[2] However, except for obvious *morphological* features such as the reentrant angle in PE (110) twins, no detailed *structural* information is available since no experimental technique can "see" the molecular stems of these beam-sensitive polymers. Molecular modeling has been used to gain some insight into the structure of the twin plane of polyethylene, but the conclusions cannot be confronted with experimental evidence.

Insights in the twin plane structure of PVCH have become possible thanks to the existence of polysynthetic twins and the associated streaking of the diffraction pattern. Similar streaked patterns have been recorded for crystals of syndiotactic polystyrene (sPS) in its β crystal modification and have been analyzed in great detail by Tsuji and collaborators.[10,11] These authors have also recorded high-resolution bright-field images of the βsPS crystals that are more beam-resistant than PVCH due to the delocalization of electrons in the aromatic ring. The HRTEM images display indeed a very dense array of twin planes oriented normal to the growth front.

Impact of Twinning on Crystallization Rates. The detailed analysis of twinning in PVCH and its impact on the single-crystal structure provides an opportunity to consider in a broader context the impact of twinning on polymer crystal nucleation and growth.

The above analyses suggest that the existence of twin planes abutting on growth faces may affect the nucleation and growth processes. We recall briefly earlier evidence that suggests that a *single* twin plane can affect the secondary nucleation process in single crystals (and possibly spherulite growth).

In the classical theories of crystal growth, the slowest process is the secondary nucleation. However, the secondary nucleation may be altered or altogether suppressed when the surface is not molecularly flat. For example, growth of NaCl crystals is significantly enhanced when the growth face contains a screw dislocation, since secondary nucleation no longer intervenes in the growth mechanism.

Twin planes may contribute to generate nonplanar growth surfaces and therefore to modify the crystallization process. Their impact is best illustrated by the morphology of single crystals, since the growth rates can be directly "read" from the crystal morphology.

The polymer literature is replete with examples of faster growth rates associated with twin boundaries. A documented example of the impact of a twin plane on growth rate is the PE (110) twin. The twinned components with (110) growth faces

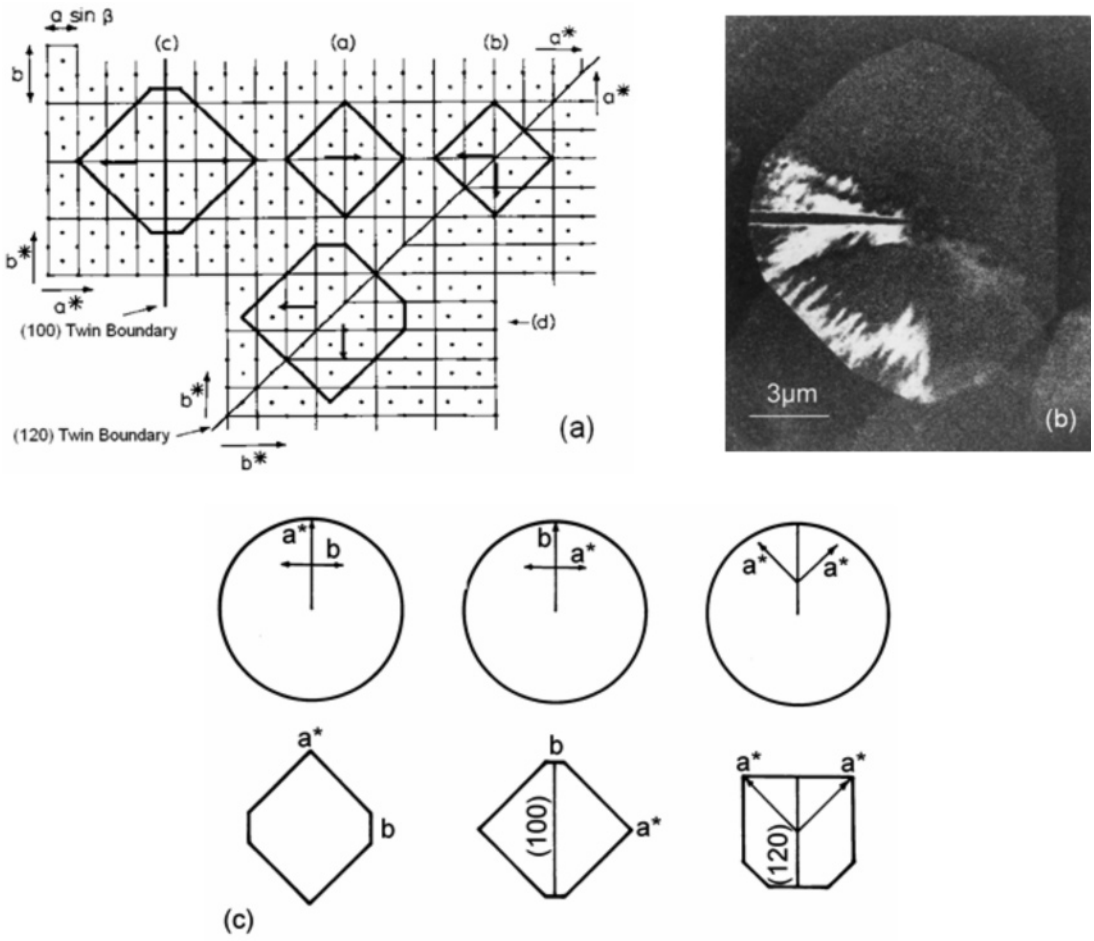

Figure 14. **(**a**)** Drawing illustrating the poly(ethylene oxide) crystal lattice, the untwinned crystal with (120) growth faces (different growth faces exist for different crystallization conditions) and the (120) and the (100) twinned crystals. Drawing reproduced and adapted from ref 2. **(**b**)** Increased growth rates at (100) twin boundaries in a single crystal of poly(ethylene oxide). The crystal displays a small microtwinned sector parallel to one its *b* axes (dark wedge oriented at 9 o'clock). The crystal is imaged in dark-field electron microscopy through one 120 diffraction spot. The increased growth rate is highlighted by comparison with the opposite, untwinned (010) growth sector. Reprinted with permission from ref 2. Copyright 1969 Dekker. **(c)** Comparison of untwinned and twinned single crystals of PEO (bottom) with the various growth directions that exist in spherulites of PEO (top).

generate a reentrant wedge that constitutes a privileged nucleation site with, in essence, two available lateral surfaces (Figure 13a). Secondary nucleation at this location does not require any extra lateral surface energy, as is the case for lateral spread. Growth along the (110) twin plane is considerably enhanced and the crystal becomes elongated (Figure 13b, taken from Wittmann and Kovacs).[3,13] By contrast, no wedge is created at the twin boundary in (310) PE twins. As a result, (310) twins and untwinned crystals have the same size.

Sticking again with PEO, Figure 14b reproduces a dark-field image of a single crystal with a twinned (100) microsector abutting on one of its (010) growth faces (dark angular sector). Of interest in the present context is the marked difference in growth rate of the two, opposite (010) growth faces of the single crystal: one of them displays, the other is free of, the (100) twin planes. Many similar observations have been made on comparable single crystals, although the differences in growth rates may be more or less marked depending on the crystallization conditions. In all cases however, the twinned sectors grow faster than the untwinned ones.

It is difficult to determine the origin of these differences in growth rates, since the detailed structural information on the (010) twin plane of PEO is missing, and twin planes are usually relatively disordered. However, the above analysis on PVCH twins may be relevant in the present context, since we are also dealing with a twin plane that abuts at right angles on a growth plane. PEO has a monoclinic unit cell with four chains that, in *c* axis projection, reduces to a square, but a face centered one (Figure 14a). If a shift of the twinned components parallel to the twin plane is created, we would again be in a situation in which secondary nucleation is modified—and actually enhanced. The details of the process are however difficult to work out in the present case.

In a broader perspective, differences in growth rates contribute to the polymorphism of polymer spherulites. Numerous crystalline polymers form different spherulites as a function of crystallization temperature. The spherulites display the same crystal structure and differ only by their radial direction, which is associated with their faster growth direction. In PEO again, radial directions can be the *a** axis, the *b* axis, or the ⟨120⟩ direction.[16] In polyethylene adipate, the radial growth directions are the *a** axis, the *b* axis, and the ⟨110⟩ direction.[17,18] We note that, besides "normal" or expected crystallographic directions that correspond to major unit-cell axes, the additional growth directions correspond to twin planes for these polymers (for PEO, the *b* axis is also parallel to a twin plane) (Figure 14c). It might be worth examining to what extent the increased growth rates associated with twinning can explain these specific radial growth directions: in other words, the radial growth directions of polymer spherulites may be the "normal" crystallographic

axes *and/or* one or several of the twin planes, the latter being best revealed by analysis of their single crystals, as has been performed here for PVCH.

Impact of Polysynthetic Twinning on Crystallization Rates. The existence of multiple twin planes affects the pattern of nucleation and growth in PVCH single crystals, which blurs the usual distinction between different growth regimes. Whereas secondary nucleation is eased, the high density of twin planes provides a structural limitation to lateral spread on the growth face. For very high densities of twin planes, the contribution of fractional secondary nucleation (lateral energy, $\sigma_{lat}bl$) to the "filling in" of the growth face reverses from enhancing the growth rate when it competes with "conventional" secondary nucleation ($2\sigma_{lat}bl$) to limiting the growth rate when competing with the lateral spread (no lateral surface energy). Since the density of twin planes increases with crystallization time, the center parts of the growth faces are the "oldest", with a high density of twin planes, and grow slower. Growth near the corners of the crystal takes always place on relatively "young" parts of the crystal, with a lower density of twin planes (cf. the essentially untwinned domains extending near the diagonals of the crystal, Figures 5 and 11). When generation of twin planes is significantly higher, the growth rates become more uniform along the growth face, and the crystals are essentially square (cf. Figures 6 and 7 for crystals grown in squalane and phenyldecane, respectively).

The above observations can equally well be described within the frame of growth regimes. The growth regimes as defined by Lauritzen and Hoffman differ essentially by the different impact of secondary nucleation and lateral spread on a growth face. Very qualitatively speaking, regimes I, II, and III correspond to a single, to multiple, and to a very high density of secondary nucleation events on the growth face. As a result, growth regimes are defined (possibly better defined) by the distances over which lateral spread contributes to the completion of the growth faces. Lateral spread extends over the whole face, over a smaller fraction of that face (the range is still debated), and over distances that approach the interstem distances for regimes I, II, and III, respectively.

Twin planes in PVCH crystals generate structural "defects" that limit the lateral spread. Since the dimensions of the twinned domains can be very small, the conventional distinction between growth regimes loses some of its relevance. For example, growth under regime I conditions would follow regime II kinetics when multiple twin planes exist on a growth face. Since twinned domains can be as little as ≈30 nm wide, growth may even be not far removed from regime III (the roughness of the growth face induced by the multiple twin planes contributes to the analogy). In other words, the conventional distinction between regimes I, II, and even III becomes blurred, since it no longer depends on relative secondary nucleation rate and lateral spread rate, but rather on the density of twin planes. This density depends on the crystallization conditions. It varies also with time and location on the growth front, since new twin planes are generated during growth. A continuum of growth regimes is "scanned" during growth of these PVCH single crystals.

Conclusion

Single crystals of PVCH have been investigated as a function of crystallization conditions. At high T_c and from the melt, single crystals and twinned crystals are formed. They are mostly growth twins. When formed in squalane or phenyldecane solution, the crystals are polysynthetic growth twins with elongated domains oriented perpendicular to the growth faces. As revealed by dark-field imaging, the domain width can be as little as a few tens of nanometers.

The polysynthetic twins yield streaked diffraction patterns that help analysis of the details of the stem organization along the twin plane. The twinned components are shifted parallel to the twin plane by one-quarter of a cell edge, i.e., by half a stem width. For twin planes abutting on a growth face, this stagger results in the formation of a jagged growth face.

As indicated by the preservation during growth of the twin planes abutting on the growth face, the existence of jagged growth faces modifies the nucleation and growth process. Our analysis suggests that the twin planes are preferred secondary nucleation sites and that the completion of the growth face through lateral spread can take place only up to the next twin boundary, where it is interrupted.

Preferred secondary nucleation at the twin plane, that is, at a site where the depositing stem takes advantage of the advancing growth front (by half a growth layer thickness), introduces the novel concept of "*fractional secondary nucleation*", i.e., of a secondary nucleation process for which the lateral surface energy barrier is lower than that associated with "conventional" secondary nucleation. On the jagged growth faces, lateral spread extends only up to the nearby twin plane. Since the contribution to growth of fractional secondary nucleation is increased and that of lateral spread is limited by structural features, the usual distinction of different growth regimes is blurred when dealing with PVCH polysynthetic twinned crystals.

Acknowledgment. A.K. thanks the Ritsumeikan University for the financial support of his sabbatical leave at CNRS-ULP, Strasbourg. We are indebted to the reviewers for useful comments.

References and Notes

(1) Agar, A. W.; Frank, A.; Keller, A. *Philos. Mag.* **1959**, *4*, 32. Reneker, D. H.; Geil, P. H. *J. Appl. Phys.* **1960**, *31*, 1916. Niegisch, W. D.; Swan, P. R. *J. Appl. Phys.* **1960**, *31*, 1906. Keller, A. *Rep. Prog. Phys.* **1968**, *31*, 623. Geil, P. H. *Polymer Single Crystals*; Interscience, a division of John Wiley & Sons: New York, London, Sydney, 1963, Chapter II, pp 79−188.

(2) Kovacs, A. J.; Lotz, B.; Keller, A. *J. Macromol. Sci., Phys.* **1969**, *B3*, 385.

(3) Wittmann, J. C.; Kovacs, A. *Ber. Bunsen−Ges. Phys. Chem.* **1970**, *74*, 901. Lotz, B.; Wittmann, J. C. In *Materials Science and Technology, Structure and Properties of Polymers*; Cahn, R. W., Haasen, P., Kramer, E. J., Eds.; VCH: Weinheim, Germany, 1993; Vol. 12, Ch. 3, pp 79−151.

(4) Pradère, P.; Revol, J. F.; Manley, R. St. J. *Macromolecules* **1988**, *21*, 2747.

(5) De Rosa, C.; Borriello, A. M.; Venditto, V.; Corradini, P. *Macromolecules* **1994**, *27*, 3864.

(6) De Rosa, C.; Borriello, A. M.; Corradini, P. *Macromolecules* **1996**, *29*, 6323.

(7) Nishikawa, Y.; Murakami, S.; Kohjiya, S.; Kawaguchi, A. *Macromolecules* **1996**, *29*, 5558.

(8) Khoury, F.; Barnes, J. D. *J. Res. Natl. Bur. Stand.* **1972**, *76A*, 225; **1974**, *78A*, 95. Barnes, J. D.; Khoury, F. *J. Res. Natl. Bur. Stand.* **1974**, *78A*, 363.

(9) Lotz, B.; Lovinger, A. J.; Cais, R. E. *Macromolecules* **1988**, *21*, 2375. Lovinger, A. J.; Lotz, B.; Davis, D. D.; Padden, F. J., Jr. *Macromolecules* **1993**, *26*, 3494.

(10) De Rosa, C.; Rapacciulo, M.; Guerra, G.; Petraccone, V.; Corradini, P. *Polymer* **1992**, *33*, 1423. Tsuji, M.; Okihara, T.; Tosaka, M.; Kawaguchi, A.; Katayama, K. *Microsc. Soc. Am. Bull.* **1993**, *23*, 57. Tosaka, M.; Hamada, N.; Tsuji, M.; Kohjiya, S. *Macromolecules* **1997**, *30*, 6592.

(11) Tosaka, M.; Tsuji, M.; Cartier, L.; Lotz, B.; Kohjiya, S.; Ogawa, T.; Isoda S.; Kobayashi, T. *Polymer* **1998**, *39*, 5273. Tosaka, M.; Tsuji, M.; Kohjiya, S.; Cartier, L.; Lotz, B. *Macromolecules* **1999**, *32*, 4905.

(12) Hoffman, J. D.; Davis, G. T.; Lauritzen, J. I., Jr. In *Treatise on Solid State Chemistry*; Hannay, N. B., Ed.; Plenum Press: London, 1976; Vol. 3, pp 497−614.
(13) Khoury, F.; Padden F. J., Jr. *J. Polym. Sci.* **1960**, *47*, 455.
(14) Burbank, R. D. *Bell Syst. Tech. J.* **1960**, *39*, 1627. Cited in: Geil, P. H. *Polymer Single Crystals*; Interscience: 1963; Chapter II, p 152.
(15) Geil, P. H.; Kiho, H.; Peterlin, A. *J. Polym. Sci., Part B: Polym. Lett.* **1964**, *2*, 71.
(16) Price, F. P.; Kilb, R. W. *J. Polym. Sci.* **1962**, *57*, 395. Balta Calleja, F. C.; Frank, A.; Keller, A. *Kolloid. Z. Z. Polym.* **1966**, *209*, 128.
(17) Point, J. J. *Bull. Acad. R. Belg.* **1953**, *39*, 435; **1955**, *41*, 974.
(18) Takayanagi, M. *Mem. Fac. Eng. Kyushu Univ.* **1957**, *16*, 111. Takayanagi M.; Yamashita, T. *J. Polym. Sci.* **1956**, *22*, 552.

MA0523217